Conjugative plasmids interact with insertion sequences to shape the horizontal transfer of antimicrobial resistance genes

You Che[a], Yu Yang[a], Xiaoqing Xu[a], Karel Břinda[b,c], Martin F. Polz[d,e], William P. Hanage[c], and Tong Zhang[a,1]

[a]Environmental Microbiome Engineering and Biotechnology Laboratory, Department of Civil Engineering, The University of Hong Kong, Hong Kong, China; [b]Department of Biomedical Informatics, Harvard Medical School, Boston, MA 02115; [c]Center for Communicable Disease Dynamics, Department of Epidemiology, Harvard T. H. Chan School of Public Health, Harvard University, Boston, MA 02115; [d]Department of Civil and Environmental Engineering, Massachusetts Institute of Technology, Cambridge, MA 02139; and [e]Department of Microbial Ecology, Centre for Microbiology and Environmental Systems Science, University of Vienna, 1090 Vienna, Austria

Edited by Edward F. DeLong, University of Hawaii at Manoa, Honolulu, HI, and approved December 11, 2020 (received for review May 4, 2020)

It is well established that plasmids play an important role in the dissemination of antimicrobial resistance (AMR) genes; however, little is known about the role of the underlying interactions between different plasmid categories and other mobile genetic elements (MGEs) in shaping the promiscuous spread of AMR genes. Here, we developed a tool designed for plasmid classification, AMR gene annotation, and plasmid visualization and found that most plasmid-borne AMR genes, including those localized on class 1 integrons, are enriched in conjugative plasmids. Notably, we report the discovery and characterization of a massive insertion sequence (IS)-associated AMR gene transfer network (245 combinations covering 59 AMR gene subtypes and 53 ISs) linking conjugative plasmids and phylogenetically distant pathogens, suggesting a general evolutionary mechanism for the horizontal transfer of AMR genes mediated by the interaction between conjugative plasmids and ISs. Moreover, our experimental results confirmed the importance of the observed interactions in aiding the horizontal transfer and expanding the genetic range of AMR genes within complex microbial communities.

antimicrobial resistance | mobile genetic elements | horizontal gene transfer | whole genome | long-reads sequencing

Antimicrobial resistance (AMR) threatens the effective treatment of an ever-increasing range of infections due to the continued evolution and widespread dissemination of antibiotic-resistant pathogens (ARPs) (1, 2). Plasmids serve as an important platform on which gene arrays are accreted and reassorted, thus playing a central role in the capture and dissemination of a variety of AMR genes (3–5). Although the classification of plasmids into three categories (i.e., conjugative, mobilizable (MOB), and nonmobilizable) on the basis of protein machinery associated with DNA transfer, including relaxase, type IV coupling protein (T4CP), and type IV secretion systems (T4SSs) has been well described (6–11), automatic tools for plasmid classification and the establishment of epidemiological links between plasmid mobility and AMR genes are strongly needed. MOB-typer (12, 13) is the state-of-the-art tool providing in silico plasmid classification but offering no information regarding antimicrobial resistance.

The occurrence, distribution, and genetic organization of AMR genes among plasmids have been documented (14–16); however, the interactions of plasmids and additional mobile genetic elements (MGEs), such as integrons (17) and insertion sequences (ISs) (18), within complex communities are not well understood, nor how these affect the spread of AMR genes. Here, we ask 1) whether the AMR gene pool is homogeneously distributed or constrained by different plasmid categories; 2) what necessary genetic elements are needed beyond plasmids for the effective and extensive horizontal transfer of AMR genes across different genetic backgrounds; and 3) how the interaction of different MGEs successfully facilitate the horizontal transfer and expand the genetic range of AMR genes in complex bacterial communities.

To address these questions, we developed a tool (Plascad) for plasmid classification (based on plasmid mobility properties), AMR gene annotation, and plasmid visualization and then determined the recent horizontal transfer network of AMR genes and the associated MGEs by systematic genetic analysis of a large collection of complete bacterial genomes (12,059) and plasmids (14,029). We found that most plasmid-borne AMR genes, including those localized on class 1 integrons, are enriched in conjugative plasmids. We provide robust evidence for the massive, IS-associated exchange network of AMR genes connecting conjugative plasmids and phylogenetically distant pathogens, suggesting a general mechanism that drives the extensive horizontal transfer of AMR genes. Finally, we used in vitro experimental approaches to reconstruct the transfer pathways of a gentamicin resistance gene (*accC1*) across various genetic backgrounds and confirmed the significance of interaction between conjugative plasmids and ISs in mediating horizontal transfer and expanding the genetic range of AMR genes in the complex bacterial communities. This study reveals the significant contributors and mechanisms responsible for the dissemination of AMR genes and highlights the need for routine surveillance to capture the dynamic

Significance

There is great interest in understanding how antibiotic resistance is disseminated by MGEs (i.e., plasmids, insertion sequences, and integrons). We have systematically investigated their interactions in mediating the horizontal transfer of resistance by combining in silico genomic analysis of a large collection of complete bacterial plasmids (14,029) and genomes (12,059), and then confirmed the interactions we observe in nature using direct experimental approaches. We showed a whole picture of all the IS-associated transfer patterns of AMR genes across different genetic backgrounds and our results highlight the significant relationships between conjugative plasmids and ISs in shaping the dissemination of AMR genes.

Author contributions: Y.C. and T.Z. designed research; Y.C. performed research; Y.C., Y.Y., X.X., and T.Z. analyzed data; K.B., M.F.P., and W.P.H. provided valuable advice on data analysis; Y.C. and T.Z. developed the bioinformatic tool; and Y.C. and T.Z. wrote the paper with advice from K.B., M.F.P., and W.P.H. and approval of all authors.

The authors declare no competing interest.

This article is a PNAS Direct Submission.

[1]To whom correspondence may be addressed. Email: zhangt@hku.hk.

This article contains supporting information online at https://www.pnas.org/lookup/suppl/doi:10.1073/pnas.2008731118/-/DCSupplemental.

Published February 1, 2021.

genetic context of AMR genes as a means to facilitate the understanding and control of this critical public health threat.

Results

AMR Genes Are Enriched in Conjugative Plasmids. To explore the relationships between different plasmid categories and the distribution pattern of AMR genes within the plasmid database, we first developed a tool not only for plasmid classification, but also for AMR gene identification and plasmid visualization (Plascad). Specifically, we classified the plasmids (14,029 in total) into three categories based on the relaxase types (MOBs) and mating pair formation (MPF) classes, with the most

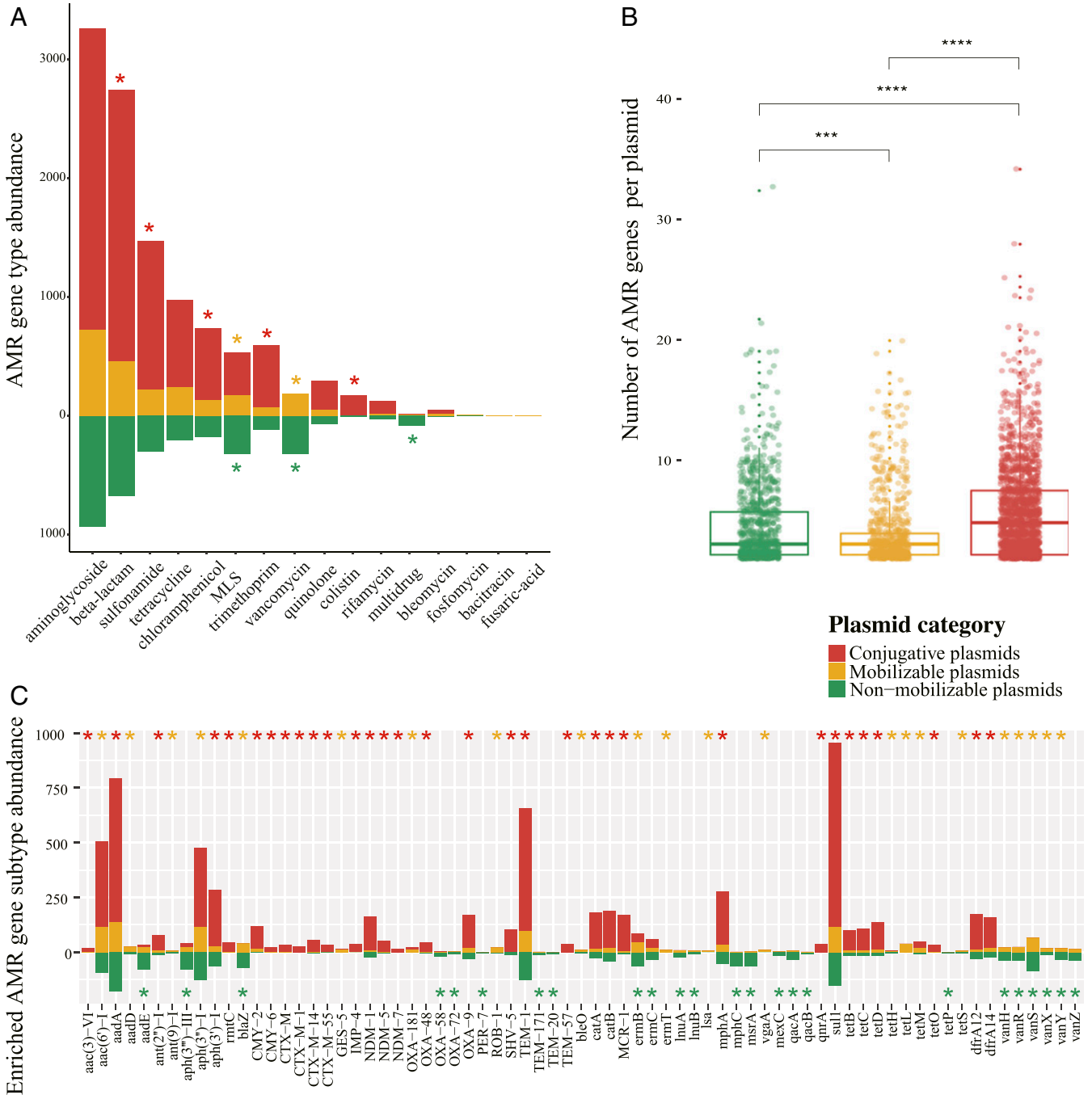

Fig. 1. Enrichment of AMR genes on conjugative plasmids. (*A*) Prevalence and abundance of all the identified AMR gene types present across three plasmid categories. Diverging barchart (up: mobilizable plasmids and conjugative plasmids; down: nonmobilizable plasmids) was plotted. Asterisks with different colors indicate AMR gene types that are significantly enriched in different plasmid categories ($P < 0.01$, OR > 1); *P* value for enrichment analysis is based on FDR-corrected (Benjamini–Hochberg) Fisher exact test. (*B*) Number of AMR genes across three categories of AMR gene-carrying plasmids. Statistical analysis is performed based on Kruskal–Wallis test followed by FDR-corrected (Benjamini–Hochberg) Dunnett's multiple-comparison test (***$P < 0.01$, ****$P < 0.001$). (*C*) Abundance of the enriched AMR gene subtypes across three plasmid categories. Asterisks with different colors indicate AMR gene subtypes that are significantly enriched in different plasmid categories ($P < 0.01$, OR > 1); *P* value for enrichment analysis is based on FDR-corrected (Benjamini–Hochberg) Fisher exact test.

abundant being members of nonmobilizable plasmids (47.6%), followed by mobilizable plasmids (27.2%), and conjugative plasmids (25.2%) (*SI Appendix*, Table S1 and Dataset S1). This tool performed well in classifying the plasmids (conjugative plasmids: sensitivity [Sn] = 95.5%, specificity [Sp] = 100%, positive predictive value [PPV] = 100%; mobilizable plasmids: Sn = 100%, Sp = 96.3%, PPV = 88.0%; nonmobilizable plasmids: Sn = 97.4%, Sp = 100%, PPV = 100%) based on a comparison with an experimentally verified benchmark dataset (Dataset S2; for workflow of Plascad, see *SI Appendix*, Fig. S1). We further compared the performance of Plascad with MOB-typer using the benchmark dataset and the result showed that Plascad performs better than MOB-typer (*SI Appendix*, Table S2).

The large size (average [avg.] 150 kb) and high GC content (avg. 50.7%) of the conjugative plasmids contrasted strikingly with those of the other two categories (*SI Appendix*, Fig. S2, Kruskal–Wallis test followed by Dunn's multiple comparison test, $P < 0.001$). These observations are consistent with previous reports (19) and may reflect the differences in the evolutionary process of different plasmid categories. Despite the relatively low abundance of conjugative plasmids, we found that AMR gene-bearing plasmids were significantly enriched in this category (*SI Appendix*, Table S1, Fisher's exact test, $P < 0.01$, odds ratio [OR] > 1). A total of 13,899 AMR genes were detected in all plasmids, and of the 16 types, most were detected in all three plasmid categories (Fig. 1*A*). However, the number of AMR genes per plasmid was variable across categories (Fig. 1*B*, avg. conjugative plasmids: 4.7; mobilizable plasmids: 2.7; nonmobilizable plasmids: 3.5; Kruskal–Wallis test followed by Dunn's multiple comparison test, $P < 0.001$). Many AMR gene types, including beta-lactam, sulfonamide, chloramphenicol, trimethoprim, and colistin resistance genes, were significantly enriched in conjugative plasmids, whereas only multidrug resistance, a resistance type that usually includes efflux pumps on the membranes of bacteria that are not necessarily related to AMR genes (20), was significantly associated with nonmobilizable plasmids (Fig. 1*A* and Dataset S3, Fisher's exact test, $P < 0.01$, OR > 1). Importantly, we found that most variants of the New Delhi metallo-beta-lactamase, extended-spectrum β-lactamase (ESBL), and colistin-encoding genes, such as bla_{NDM} (21), $bla_{\text{CTX-M}}$ (22), and *mcr-1* (23), which have emerged as severe clinical threats, were also significantly enriched in conjugative plasmids (Fig. 1*C*), which might explain their global dissemination.

Conjugative Plasmids Play a Central Role in Mediating the Transfer of AMR Genes across Plasmid Categories and Distant Phylogenetic Lineages. We further examined the distribution of the dominant AMR gene subtypes (top 50, accounting for more than 90% of its total number) identified on conjugative plasmids and found that most of these subtypes (94%) were widely distributed in the other two plasmid categories with high abundance (avg. 67%) despite the considerable difference in the overall diversity composition (*SI Appendix*, Fig. S3), which indicates extensive horizontal transfer of AMR genes among different plasmid categories. To elucidate the extent of genetic exchange and major contributors to the transfer of AMR genes among all AMR gene-bearing plasmids, we constructed a bipartite network connecting the plasmids and AMR genes (*SI Appendix*, Fig. S4); when an AMR gene was transferred between two plasmids, both plasmids were linked to the AMR gene by edges. Nodes and edges were organized using the ForceAtlas2 algorithm (24). We asked whether there exist barriers for the horizontal transfer of AMR genes carried by the nonconjugative plasmids; a well mixing together of plasmid communities would be expected if no barrier exists. We observed a large hub of strongly connected conjugative plasmids and some mobilizable and nonmobilizable plasmids (*SI Appendix*, Fig. S4). In contrast, relatively sparsely connected to this hub were many nonconjugative plasmids that carried some AMR genes associated with vancomycin, macrolide-lincosamide-streptogramin (MLS), and multidrug resistance, which were rarely found in conjugative plasmids, suggesting that there indeed exist barriers for the horizontal transfer of AMR genes mediated by these plasmids and highlighting the significant role of conjugative plasmids in promoting the horizontal transfer of AMR genes within the plasmid communities (16, 25).

To investigate the contribution of conjugative plasmids in mediating the exchange of AMR genes not only across plasmid categories but also between bacterial chromosomes, we explored the recently transferred AMR genes between conjugative plasmids and bacterial chromosomes based on a perfect nucleic acid sequence match (100% similarity). We identified a massive exchange network of 171 unique AMR genes (11 types, 83 subtypes) involving 703 bacterial genomes (19 genera, 95% were pathogens) and 1,584 conjugative plasmids (Fig. 2*A* and *SI Appendix*, Fig. S5). Of the dominant AMR gene subtypes (top 50) detected on conjugative plasmids, more than 86% were found to be transferred across bacterial genera; interestingly, a large fraction of the bacteria (65%) involved in this process were enriched with multiple resistance (Fig. 2*A*), indicating that conjugative plasmids play an important role in mediating the interspecific transfer of AMR genes, since direct transfer of chromosomal AMR genes between any two bacteria was unlikely due to the phylogenetic barriers to horizontal gene transfer (HGT) (26). In contrast, we used the same approach to explore the transfer of AMR genes that were only carried by nonmobilizable plasmids. Thirty-eight unique recently transferred AMR genes (six types, 36 subtypes) that were associated with 90 nonmobilizable plasmids and 237 bacterial genomes (five genera, 97% pathogens) were identified, and only ~10% of AMR gene subtypes can be transferred across genera (Fig. 2*B*), indicating the limited ability of these plasmids to facilitate the horizontal transfer of AMR genes across phylogenetically distant bacteria, which is supported by a recent finding (27). It is worth noting that most of the bacteria (~78%) that had undergone AMR gene transfer were isolated from ecologically similar settings (i.e., human related; Dataset S4), consistent with previous findings that HGT is strongly structured by ecology rather than geography (28). The high incidence of AMR gene transfer in human-associated pathogens may be caused by environmental and therapeutic exposure to antibiotics, as well as pervasive interactions with multidrug-resistant bacteria (29). Overall, our findings collectively provide evidence for the significant role of conjugative plasmids in facilitating the transfer of AMR genes across plasmid categories and distant phylogenetic lineages but link human-associated pathogenic bacteria globally.

The Interaction between Conjugative Plasmids and ISs Is a General Mechanism in Mediating the Transfer of AMR Genes. Given the differential roles of different plasmid categories in the transfer of AMR genes, it became essential to answer the fundamental questions regarding the necessary genetic elements beyond plasmids that allow the accumulation and extensive transfer of AMR genes across diverse genetic contexts. Therefore, we investigated whether class 1 integrons, which have been recognized as important agents that help plasmids acquire resistance determinants (30), played a role. We systematically scanned all plasmids and identified a total of 706 class 1 integrons (type A: 549 and type B: 157), most of which (73%) were localized on conjugative plasmids (*SI Appendix*, Fig. S6 *A–C*). Strikingly, while almost all (97%) of the plasmid-borne class 1 integrons carried at least one resistance gene, only 54 (18.4%) of the 293 AMR gene subtypes were integron associated, indicating that class 1 integrons only accumulate specific AMR genes on plasmids. The limited contribution of class 1 integrons to the accumulation of AMR genes was supported even when considering the AMR gene number, rather than only the diversity of integron-associated

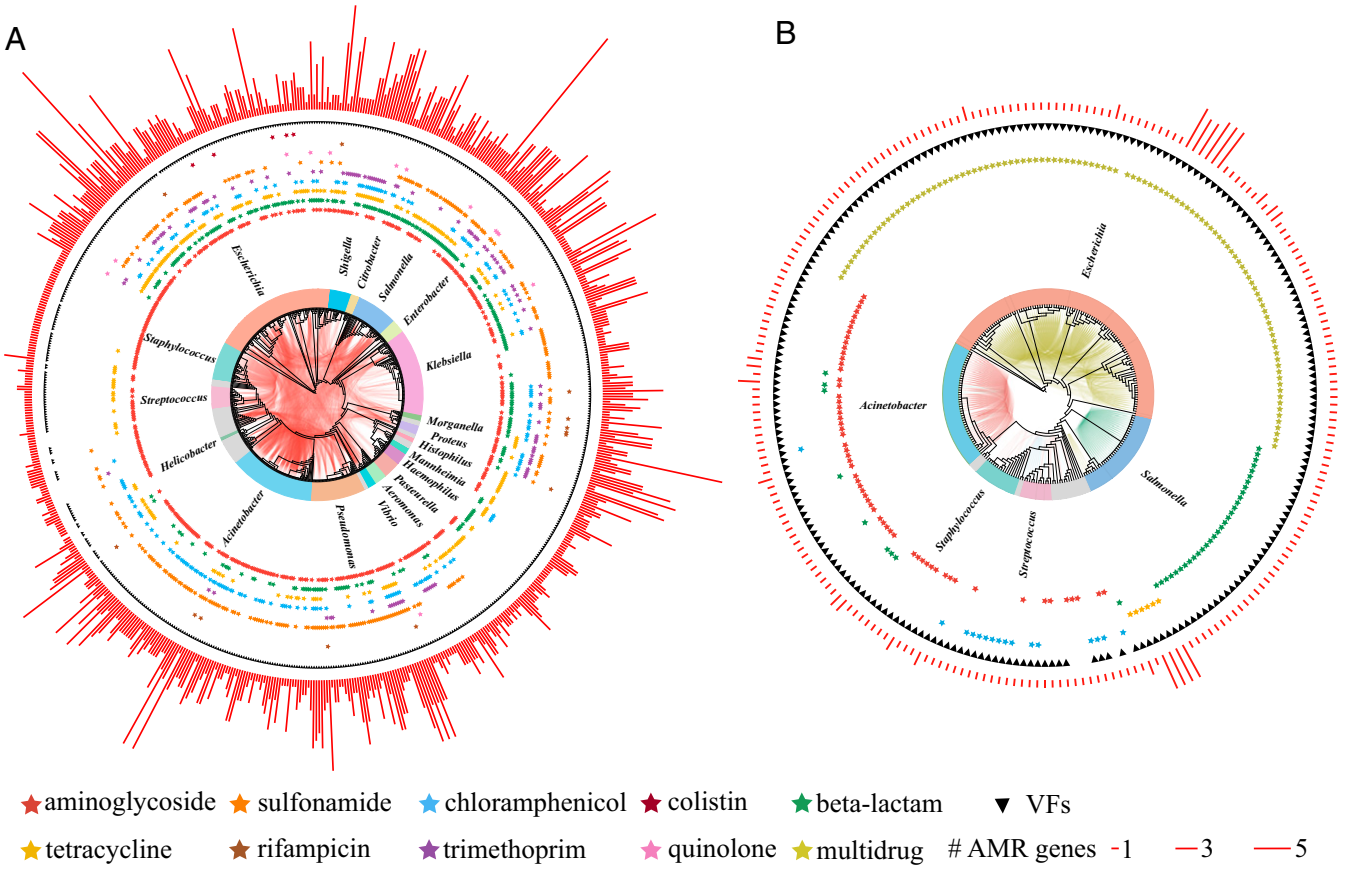

Fig. 2. Phylogenetic distribution of bacterial genomes involved in the recent horizontal transfer (100% nucleic acid identity) of AMR genes mediated by conjugative (*A*) and nonmobilizable plasmids (*B*). (*A*) Only the exchange networks of aminoglycoside genes mediated by conjugative plasmids was displayed for visualization purposes; for the remaining eight types, see *SI Appendix*, Fig. S5 *A–H*. (*B*) Limited phylogenetic range of recently transferred AMR genes (four types) mediated only by nonmobilizable plasmids. The phylogenetic trees are constructed using a multiple sequence alignment of the full 16S rRNA genes extracted from the corresponding genomes. The inner solid lines indicate the recent transfer of AMR genes among different bacteria mediated by two plasmid categories; the lines are colored according to the AMR gene types (colored asterisk) involved in the horizontal transfer. The outer triangles indicate bacteria with virulence factors, and the outmost red bars display the number of the total AMR genes carried by the corresponding bacteria.

AMR genes; only resistance types of sulfonamide (49.2%), rifamycin (61.4%), and trimethoprim (49.7%) accounted for a relatively high proportion among all plasmid-borne AMR genes (*SI Appendix*, Fig. S6*C*). These results indicate the commitment of large-scale horizontal transfer mediated by other mechanisms rather than integron-mediated site-specific recombination in generating the communal dynamic AMR gene pool.

We then investigated whether ISs, which are known to play an important role in genome evolution and plasticity (31, 32), were associated with these processes. We found that ISs were more prevalent and present at a higher abundance (Kruskal–Wallis with Dunn's multiple comparison test, $P < 0.001$) on conjugative plasmids (78.6%, avg. 6.6, average for plasmids that carry at least one IS) than on plasmids from the other two categories (42.7%, avg. 6.2 and 32.3%, avg. 5.3 for mobilizable and nonmobilizable plasmids, respectively; Fig. 3*A*). We subsequently focused on plasmids carrying AMR genes and discovered that there were more ISs on AMR gene-bearing plasmids than on those without AMR genes, regardless of plasmid category (Fig. 3*B*, Kruskal–Wallis with Dunn's multiple comparison test, $P < 0.001$), and this association was further confirmed by Pearson's χ^2 test ($P < 2.2e^{-16}$). Moreover, we found that the regions around AMR genes (5 kb upstream and downstream) had a higher density of ISs than nonadjacent regions (Fig. 3*C*, Kruskal–Wallis with Dunn's multiple comparison test, $P < 0.001$), clearly indicating the contribution of ISs to the accumulation of AMR genes on plasmid. In addition, a significant positive correlation (Pearson's correlation test, $R^2 > 0.95$, $P < 0.001$) between the prevalence and total abundance of ISs across all plasmids was observed, which revealed that some ISs were widespread, such as the extraordinarily abundant IS26 (Fig. 3*D*). Although the detected ISs were highly diverse (28 families), most of the prevalent (top 15) ISs were carried by conjugative plasmids (avg. 72.6%), as highlighted in Fig. 3*D*. To further investigate the associations between AMR genes and ISs on the plasmids, the adjacent fragments, i.e., 5 kb upstream and downstream of all the AMR genes, were examined. Interestingly, we found that ISs were closely associated with nearly all AMR gene types, as evidenced by the ratio of IS-associated AMR genes (more than 77.1% in terms of number) to total plasmid-borne AMR genes (Fig. 4). Overall, these results strongly suggest the significant role of ISs in the recruitment and transfer of AMR genes.

To test these findings, the adjacent ISs (i.e., 5 kb) of the recently transferred AMR genes between conjugative plasmids and bacterial chromosomes were investigated. All genomic pairs sharing >97% average nucleotide identity (ANI) were deduplicated (33) to avoid overcounting the horizontal transfer of IS-associated AMR genes that were potentially vertically related. Notably, we discovered a broad (245 pairs), IS-associated (identical AMR genes with the same flanking ISs) AMR gene transfer network linking the conjugative plasmids and the bacterial chromosomes (Fig. 5*A* and *SI Appendix*, Figs. S7–S16 for each of the 11 AMR

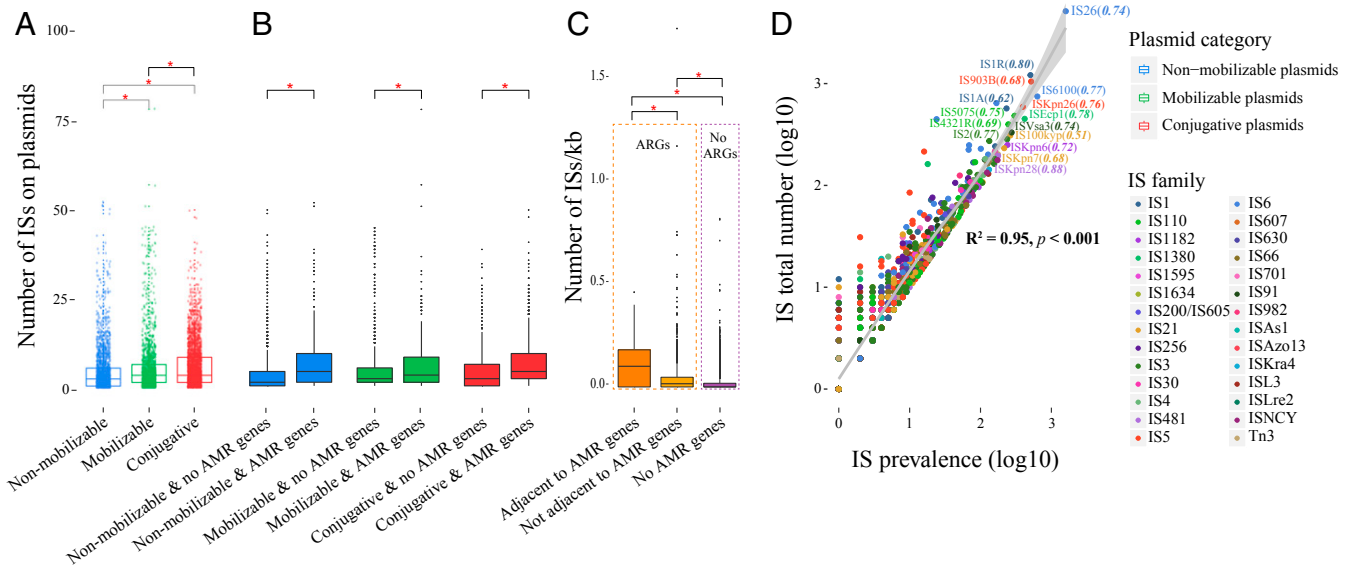

Fig. 3. Enrichment of ISs on AMR gene-bearing plasmids. (*A*) A boxplot is plotted showing the number of ISs in three plasmid categories. Statistical analysis was performed using the Kruskal–Wallis test followed by FDR-corrected (Benjamini–Hochberg) Dunn's multiple comparison test (*$P < 0.001$). (*B*) A pairwise boxplot is plotted showing the differences in IS abundance between AMR gene-bearing plasmids and those without AMR genes in each of the plasmid categories. *P* value based on FDR-corrected (Benjamini–Hochberg) Mann–Whitney test (*$P < 0.001$). (*C*) IS density in AMR gene-bearing plasmids and those without AMR genes (regions adjacent to AMR genes are defined as 5 kb upstream and downstream of the AMR genes). Statistical analysis is performed using the Kruskal–Wallis test followed by FDR-corrected (Benjamini–Hochberg) Dunn's multiple comparison test (*$P < 0.001$). (*D*) Prevalence and total number of ISs present in all plasmids. The most prevalent 15 ISs are highlighted with labels, and the number in brackets indicates the proportion of ISs characterized in conjugative plasmids. ISs are colored according to their broad family categories. The linear regression lines with 95% confidence interval (shaded areas) were derived from Pearson's correlation analysis. Values are plotted on a logarithmic scale.

gene types), large enough to cover most (71% subtypes) of the transferred AMR genes that we detected above. The above finding prompted us to investigate the extent to which ISs are also involved in the transfer of AMR genes in the other two plasmid categories. Indeed, 70% of the IS-AMR gene combinations were also observed in the other two plasmid categories (*SI Appendix*, Fig. S17 *A* and *B* for mobilizable and nonmobilizable plasmids, respectively). Furthermore, some horizontally transferred AMR gene-bearing class 1 integrons were also flanked by the same ISs, with the most prevalent gene cluster containing the *intI1*, *drfA*, *aadA*, and *sul1* genes (*SI Appendix*, Fig. S18), indicating the significant role of ISs in mediating the transfer of AMR genes, even AMR gene clusters, across different genetic contexts. In summary, we showed that a majority (63.2%) of the recently transferred AMR genes between plasmids and bacterial chromosomes can be attributed to ISs (Dataset S5). Notably, a relatively small group of bacterial pathogens belonging to the notorious ESKAPE panel (except for *Enterococcus faecium* and *Staphylococcus aureus*) (34) and World Health Organization (WHO) priority pathogens list, such as *Klebsiella pneumoniae*, *Acinetobacter baumannii*, *Pseudomonas aeruginosa*, *Enterobacter* spp., *Shigella* spp., *Salmonella enterica*, and *Escherichia coli*, accounted for a large fraction of the total IS-associated transfer events, although the available genomes are probably enriched for pathogens (Fig. 5*B*).

Although the importance of ISs in the dissemination of resistance, including in plasmids, has been previously underlined by multiple studies (35–38), the links between plasmids, ISs, and AMR genes was systematically addressed in this paper, comprehensively exposing specific connections and the transfer range of these links. Specifically, among the 59 IS-associated AMR gene subtypes transferred between conjugative plasmids and bacterial chromosomes, 41 were found to be associated with more than one type of IS, with the most promiscuous occurring with IS26, which was involved in the transfer of 33 AMR gene subtypes (10 types), followed by ISEcp1 (16 subtypes, 5 types), and IS6100 (10 subtypes, 7 types), suggesting that these ISs are more successful than others in mediating the transfer of AMR genes (Fig. 5). Of greatest concern, we found that ISs were closely involved in the transfer of New Delhi metallo-beta-lactamase (e.g., ISAba125-$bla_{\text{NDM-1}}$), extended-spectrum β-lactamase (e.g., ISEcp1/IS26-$bla_{\text{CTX-M}}$), and colistin-encoding (e.g., ISApl1-*mcr-1*) genes between different genetic backgrounds (Fig. 6). The association between ISApl1 with *mcr-1* was also supported by previous findings (23). Interestingly, the completeness of the flanking ISs varied considerably for many horizontally transferred AMR genes (*SI Appendix*, Figs. S7–S16), ranging from mutations with only partially decreased length (for example, the ISEcp1-associated $bla_{\text{CTX-M}}$ and bla_{CMY} genes, *SI Appendix*, Fig. S8) to others that lost the ISs completely (for example, the loss of ISApl1 for some *mcr-1* genes, Fig. 6), suggesting that stabilization of the transferred AMR genes may be caused by dynamic mutation or deletion of the flanking ISs.

Direct Experimental Approaches Confirm the Significance of Interaction between Conjugative Plasmids and ISs in Mediating the Transfer and Expanding the Genetic Range of AMR Genes within Complex Microbial Communities. Finally, we confirmed the importance of the proposed mechanism in mediating the horizontal transfer and expanding the genetic range of AMR genes in complex environmental microbial communities. We experimentally reproduced the transfer pathway of a gentamicin resistance gene *accC1* (Gm^R) and tracked its fate in the microbial communities of two wastewater treatment plants (WWTPs). As an important and unique interface between humans and environments, WWTPs provide an ideal environment for the exchange of genetic materials associated with various adaptive traits, potentially leading to the emergence and spread of human MDR pathogens. We chose IS26 as a representative IS, given its close association with a wide variety of AMR genes. We used *Escherichia coli* DH5α that contains the nonmobilizable plasmid

Fig. 4. Close association between AMR genes and ISs. A scatter pie chart is plotted showing the associations of AMR genes with the adjacent ISs (5 kb upstream and downstream of the AMR genes) in all plasmids (red: conjugative plasmids; green: mobilizable plasmids; blue: nonmobilizable plasmids). The *Top* barchart indicates the number of AMR genes that are associated (red) or not associated (blue) with ISs, and the percentages (%) represent the ratios of IS-associated AMR genes for each AMR type. Circle size indicates the number of AMR genes in each AMR type that are associated with the corresponding ISs on the *Left*.

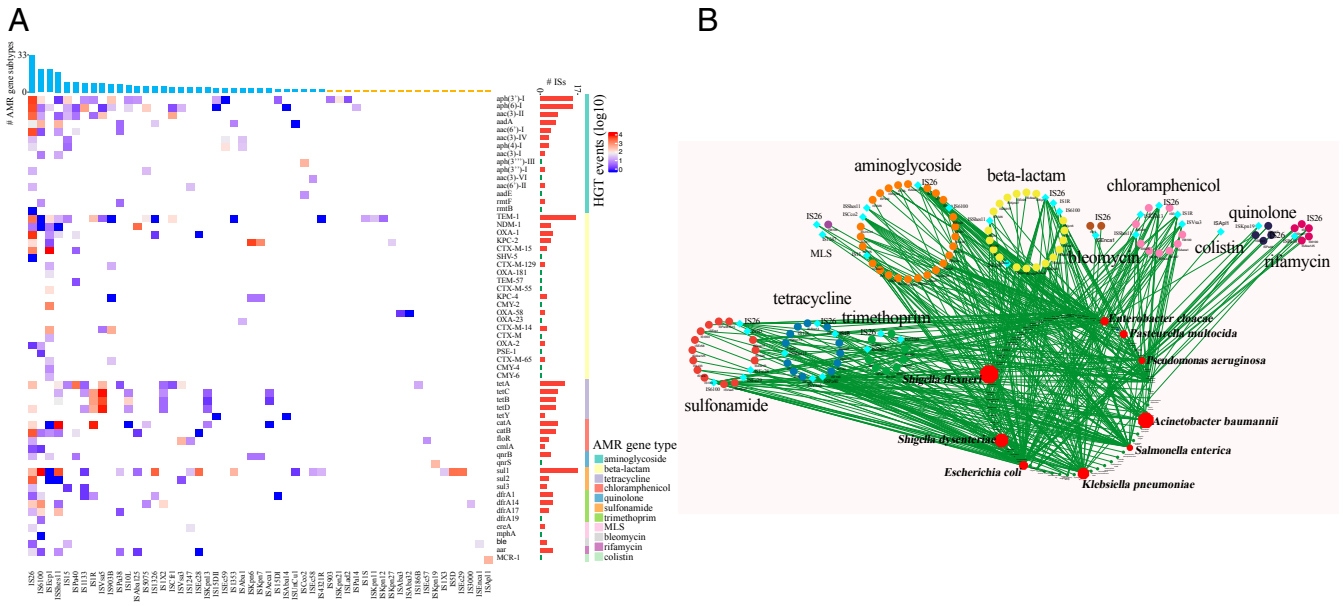

Fig. 5. ISs are an important force in shaping the recent AMR gene transfer between conjugative plasmids and bacterial chromosomes. (*A*) A heat map is plotted showing the IS-associated AMR gene transfer patterns (245 combinations) across conjugative plasmids and bacterial chromosomes. *Top* barchart indicates the number of transferred AMR gene subtypes that are associated with the corresponding ISs. *Right* barchart indicates the number of ISs that are associated with the corresponding AMR gene subtypes. Yellow and green bars indicate transfer events with abundance equal to one. The *Rightmost* bars are colored according to the AMR gene type they represent. (*B*) A network map is plotted showing the distributions of bacteria that are involved in the horizontal transfer of IS-associated AMR genes (totaling 11 types) with conjugative plasmids. Cyan diamonds denote the dominant ISs involved for each AMR gene type; top five dominant ISs are denoted for aminoglycoside, beta-lactam, chloramphenicol, sulfonamide, and tetracycline; top one dominant IS is denoted for MLS (IS26 and IS1247 have equal contribution), bleomycin, colistin, quinolone, rifamycin, and trimethoprim (IS26, IS6100, and ISShes11 have equal contribution). Dominant species involved in IS-associated AMR gene transfer are highlighted in red, with the size of the octagon being proportional to the number of the AMR gene transfer events after species level normalization (only species with more than 20 complete genomes are considered).

pUC57 carrying the IS26-associated Gm^+ (pUC57-IS26-Gm^+-IS26) as the original source of the Gm^R gene. We then constructed an EYFP-tagged conjugative plasmid RP4-Plac-*eyfp*-Cat^+ and conjugatively introduced it into the above *E. coli* DH5α; the transfer of IS26-associated Gm^R to this conjugative plasmid was explored by the solid-surface mating-out assay with *E. coli* K12 MC1061-Rif^+ to detect the cointegrates formed between the two plasmids.

We subsequently performed nanopore whole-genome sequencing to confirm the integration of IS26-associated Gm^R into the chromosome of the donor bacteria, as well as the EYFP-tagged RP4 plasmids. Notably, random incorporations were observed throughout the chromosome of the donor *E. coli* DH5α after ∼12 h of overnight growth (*SI Appendix*, Fig. S19*A*), and further incorporation occurred after seven cycles (one cycle of overnight growth) of repeated subcultivation (*SI Appendix*, Fig. S19 *B* and *C*). Meanwhile, we found that the IS26-associated Gm^R was incorporated randomly in EYFP-tagged RP4 plasmids based on the genetic context analysis of 11 randomly picked transconjugants (*SI Appendix*, Fig. S19*D*). These results confirmed the importance of IS26 in mediating the transfer of AMR genes across distantly related genetic backgrounds and were consistent with previous work (39). Three resulting cointegrates obtained above were then separately introduced into a red fluorescent labeled *E. coli* K12 MC1061-Rif^+::*mRuby3* by a mating assay to investigate the transfer and fate of Gm^R after further conjugation process. Whole-genome sequencing of mRuby3-expressing transconjugants showed that IS26-associated Gm^R was successfully incorporated into the chromosome (*SI Appendix*, Fig. S19 *E*–*G*), confirming the significant role of interaction between conjugative plasmids and ISs in mediating the horizontal transfer and expanding the genetic range of AMR genes (from conjugative plasmid to chromosome). These results inspired us to explore the permissiveness of the RP4 plasmids and the interaction between the RP4 plasmid and IS26 in mediating the transfer of AMR genes across different genetic backgrounds in complex bacterial communities. We further performed mating experiments between the donor bacteria (*E. coli* K12 MC1061-Rif^+::$lacI^q$-$K_m{}^+$) harboring the cointegrated RP4 plasmids (RP4-Plac-*eyfp*-cat^+-IS26-Gm^+-IS26) and an indigenous bacterial community of activated sludge (AS) collected from two WWTPs. The donor bacteria, which could inhibit the expression of RP4-borne *eyfp*, were constructed in vitro to distinguish from potential recipients. After mating, 10 colonies of EYPF-expressing transconjugant cells on Petri dishes were isolated from each of the above two mixed communities under a fluorescence microscope and sequenced. We observed the transfer of plasmids from the donor strain to a wide variety of bacteria, and 20 bacterial strains belonging to eight different genera of the *Proteobacteria* phylum were identified, with *Pseudomonas* being the most abundant genus isolated (Fig. 7). Strikingly, we found that IS26-associated Gm^R was incorporated into the chromosomes of most isolates (85%), with more than 50% having multiple insertion sites (Fig. 7; range 2 to 9, avg. 3.5), which generated a dynamic AMR gene pool that was ready for further transmission. Together, our results provided direct experimental evidence in support of the proposed general mechanism that the interaction between conjugative plasmids and ISs plays an important role in facilitating the dynamic transfer of AMR genes, broadening our understanding of the evolution and adaptation of bacterial resistance.

Discussion

In this work combining bioinformatic analysis with direct experimental approaches, we determined the key insertion sequences (e.g., IS6 family) that were closely associated with a

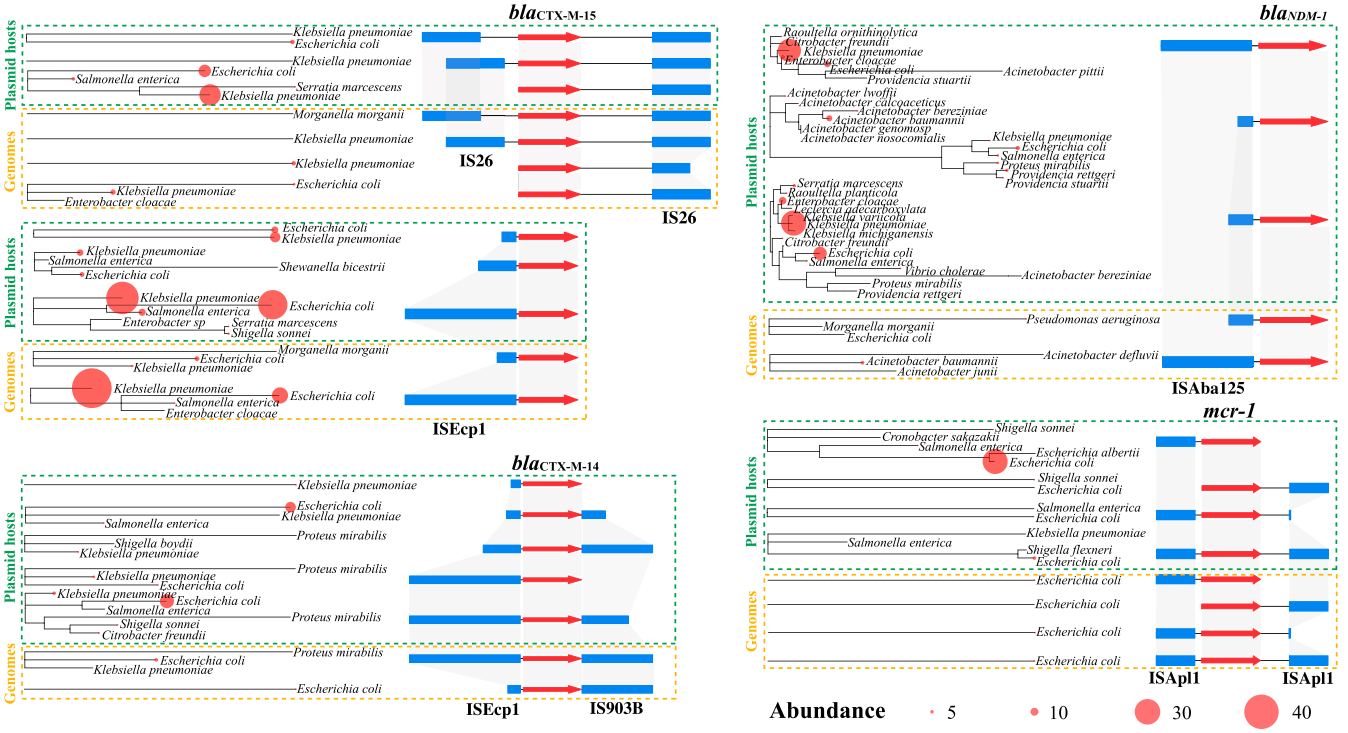

Fig. 6. A pairwise synteny comparison is plotted displaying the horizontal transfer patterns of IS-associated AMR genes ($bla_{CTX\text{-}M\text{-}14}$, $bla_{CTX\text{-}M\text{-}14}$, $bla_{NDM\text{-}1}$, and *mcr-1*) between conjugative plasmids (highlight with green dash outline) and bacterial chromosomes (highlight with yellow dash outline). Arrows in red indicate the horizontally transferred AMR gene subtypes (100% nucleic acid identity), and blue rectangles represent the associated flanking ISs (5 kb upstream and downstream). For each comparison, a phylogenetic tree was constructed using a multiple sequence alignment of the full 16S rRNA extracted from bacterial genomes and the hosts of the conjugative plasmids. The 16S alignments were performed using MUSCLE. The tree was then constructed using FastTree. The size of red dots on branches in the phylogenetic tree is proportional to the number of each bacterial species that is involved in IS-associated AMR gene transfer. Only the dominant ISs that are associated with the corresponding AMR genes are shown. For other IS-associated AMR gene transfer events, see *SI Appendix*, Fig. S7–S16.

variety of AMR genes. Moreover, we showed a whole picture of all the IS-associated transfer patterns between conjugative plasmids and chromosomes, which provided a comprehensive framework for targeting the resistance with high risk of dissemination. We found that conjugative plasmids play a central role in the enrichment of plasmid-borne AMR genes, including those localized on class 1 integrons. The mobility of conjugative plasmids should be a strong factor facilitating the accumulation of AMR genes, as these plasmids possess the ability to "visit" phylogenetically distant bacteria and undergo genetic exchange with other plasmids and bacterial chromosomes (16, 40), which was also supported by the extremely broad transfer range of these plasmids that has been demonstrated in the present and previous studies (41–43). Notably, previous research found that nonmobilizable plasmids are subject to high evolutionary turnover and are frequently transferred among *Vibrionaceae* populations (44), although their spread at the family level remains to be studied. This observation indicates the presence of diverse mechanisms mediating the dynamic transfer of plasmids in certain communities. Although the mobility of the plasmid determines the potential recipient of the AMR genes, the introduction of a plasmid into a recipient does not ensure successful transfer unless the transferred plasmid is stably maintained or integrated into the chromosome (45). Investigation of toxin-antitoxin systems (46, 47) that promote plasmid maintenance revealed that these systems were prevalent (>85% of all conjugative plasmids) and significantly enriched on conjugative plasmids (Dataset S6; Fisher's exact test, $P < 0.01$, OR > 1), which is particularly important since these addiction systems can provide longer retention times for conjugative plasmids than for other plasmid categories to capture and can lead to the accumulation of different kinds of AMR genes even in the absence of antibiotic selection.

Furthermore, we discovered an AMR gene transfer network linking human-associated pathogens and conjugative plasmids, yielding an overall estimated contribution of ~70% for the recently transferred AMR genes (except multidrug resistance-type AMR genes) between phylogenetically distant bacteria. Interestingly, although a high abundance of multidrug resistance genes has been detected in various environments (48–50), this AMR gene type was found to be exclusively enriched on nonmobilizable plasmids and showed phylogenetically constrained transfer capacity. The spread of these AMR genes may be caused by vertical or limited horizontal transfer since the major contributors to this type are not commonly specified by MGEs (51, 52). It is important to emphasize that although by conservatively defining (100% similarity) recently transferred AMR genes, we may have overestimated the frequency of recent horizontal transfer of AMR genes even genome deduplication was conducted, because the acquisition of AMR genes may have happened in the ancestral genomes; however, the introduction of the flanking ISs of the AMR genes as an additional filter can greatly reduce this risk, especially considering the dynamic evolution of ISs (*SI Appendix*, Figs. S7–S16) (18, 32).

Notably, ISs were closely associated with AMR genes and involved in the transfer of most AMR genes (>60% in terms of number) between plasmids and bacterial chromosomes, with the most noteworthy example being the interspecific transfer mediated by IS26 and IS6100, both of which belong to the IS6 family. We found that IS26 was not only enriched on plasmids (Fig. 3*D*)

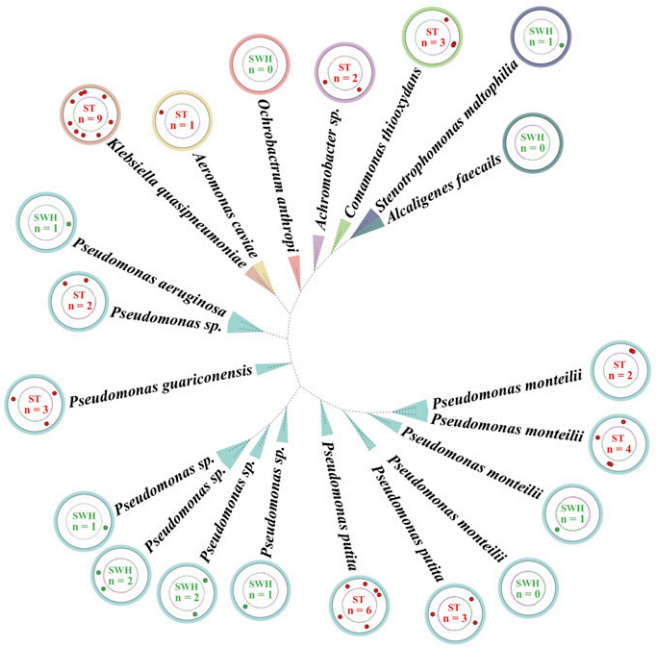

Fig. 7. Mosaic cointegrations identified on the chromosomes of the sequenced clones indicate the extraordinary capability of interaction between RP4 and IS26 to expand the genetic range of AMR genes. Fate of the IS26-associated Gm^+ carried by the cointegrated RP4 plasmids (RP4-Plac-*eyfp*-*cat*$^+$-IS26-Gm^+-IS26) after mating with the indigenous bacterial communities collected from two activated sludge samples (ST and SWH). A phylogenetic tree was constructed with 16S rRNA genes extracted from a total of 20 randomly selected transconjugants. The outermost circles represent genomes of the transconjugants, and red (ST) and green (SWH) dots indicate the cointegrated locations of the IS26-associated Gm^+ on the chromosomes of the sequenced transconjugants. The number in the innermost circle represents different integration locations.

but was widely present across diverse bacterial taxa, including at least 21 genera belonging to seven families (*SI Appendix*, Fig. S20). Thus, we speculate that the extensive distribution of IS26, as well as its efficient transfer mechanism, which has been demonstrated previously (39, 53), may operate jointly to explain its marked contribution to the transfer of AMR genes. It is reasonable to believe that AMR genes were intimately linked to conjugative plasmids and ISs, since the acquisition of plasmids may come at a fitness cost (54); however, in the presence of such numerous and dynamically distributed ISs, even transitory colonization by the conjugative plasmids could offer enough opportunities for the spread of IS-associated AMR genes across different genetic backgrounds (e.g., chromosome/intrinsic plasmids), thus allowing mitigation of the effects of the physiological burden caused by the maintenance of plasmids while maximizing the survival benefit to the hosts. It should be noted that some ISs may be in close proximity to the AMR genes; however, they are not necessarily responsible for the movement of AMR genes across different genetic backgrounds, for example, although bla_{KPC} is usually surrounded by ISKpn6 and IKSpn7, they are actually embedded in a Tn4401 transposon, which is actually responsible for the transfer events (55).

Of particular interest are the complex mutational events of the ISs, which stand in sharp contrast to the observed sequence homogeneity of the transferred AMR genes. Although these mosaic structures can be rationalized by some evolutionary balance between the advantages accrued through the acquisition of AMR genes and the deleterious effects of invasion due to the associated ISs, the factors that drive the transfer and stabilization of AMR genes by this cooperation are still unclear. The use of antibiotics may to some extent affect these processes (56, 57) and lead to persistent alterations in the genetic context of the transferred AMR genes (58); however, previous results have suggested that the contribution of antibiotics to the promotion of conjugation may be overestimated (59).

We used a culture-based approach to confirm the proposed mechanism in mediating the horizontal transfer and expanding the genetic range of AMR genes in WWTPs. We appreciate the limitations associated with the inability to cultivate a majority of the indigenous microbial community members, leading to substantial underestimation of the host range of the RP4 plasmid (41, 42). Nonetheless, it is clear that successful interaction between conjugative plasmids and ISs greatly increases the genetic range of AMR genes within complex environmental communities, as evidenced by the fact that at least one AMR gene insertion occurred on the chromosomes of 85% of the transconjugants. Most notably, the dynamic interactions between these MGEs may potentiate the evolution of multidrug-resistant pathogens with enhanced resistance via the accumulation of disparate resistance determinants in the same cell, which emphasizes the need to develop broadly applicable methods, such as real-time nanopore sequencing (60, 61), to rapidly reveal the genetic context of AMR genes before any specific intervention strategies are applied in clinical settings. It should be noted that easily cultured and pathogenic bacteria are overrepresented in the current complete plasmid and genome database and additional potential conjugative plasmids await identification and characterization. In conclusion, our findings advance the current understanding of the mode of AMR gene transfer and underscore the significant relationships between genetic interactions that shape the dissemination of AMR genes.

Materials and Methods

Complete Bacterial Plasmid and Genome Collection. An Entrez query was used for the initial retrieval of putative complete bacterial plasmid sequences from the National Center for Biotechnology Information (NCBI) nucleotide database (August 2018), and Biopython scripts were used to remove incomplete and nonplasmid sequences based on a regular expression search of descriptions in the accession titles (*SI Appendix, Supplementary Methods*). A total of 14,029 complete plasmids were compiled after removing the identical sequences. Complete bacterial genomes (12,059) were directly downloaded from the NCBI genome database (September 2018). The taxonomic lineages of both the hosts of the plasmids and the genomes were first retrieved from the GenBank files and then revised according to the Genome Taxonomy Database (GTDB) (62). The full lists of complete genomes and plasmids used in this study are summarized in Dataset S7.

Plasmid Classification, AMR Gene Detection, and Visualization Tool. We developed Plascad, a computationally efficient tool designed for automated plasmid classification, AMR gene detection, and plasmid visualization. Briefly, plasmids were classified into three categories (conjugative, mobilizable, and nonmobilizable) according to the protein machinery associated with DNA transfer, including relaxase, T4CP, and T4SSs, as suggested previously (6–9). A plasmid containing relaxase, T4CP, and T4SSs is considered a conjugative plasmid, whereas one encoding only a relaxase is called a mobilizable plasmid. To perform MOB typing, PSI-BLAST (2.3.0) (63) was conducted using eight families of N-terminal (~300 amino acid [aa]) relaxase protein sequences (6–8) (MOB_C: 1e-4, MOB_F: 1e-8, MOB_H: 1e-2, MOB_P: 1e-4, MOB_Q: 1e-4, MOB_V: 1e-2, MOB_B: 1e-4 and MOB_T: 1e-4) as queries against all the Prodigal (normal mode)-predicted open reading frames (ORFs) (64) of the complete plasmids with a maximum of 14 iterations (*SI Appendix*). To classify T4SSs into four archetypes, the major ATPase (*VirB4* and *TraU*), T4CP (*VirD4*), and four sets of well-described type-specific genes (MPF_F: *TraLEKVCWUcNHD*; MPF_G: *p31*, *p35*, *p41*, *p44*, *p51*, *p52*; MPF_I: *TraIKLMNPQRWY*; MPF_T: *VirB3689*) were considered (*SI Appendix, Supplementary Methods*). We performed a PSI-BLAST search (maximum of 30 iterations) of each key protein against the plasmid database, and then, multiple alignments coupled with phylogenetic analyses were performed for each uncovered protein family using MUSCLE (v3.8.31) (65) and

FastTree (2.1.10) (66) to remove the spurious hits (i.e., sequences with length less than 50% of the majority proteins as well as the isolated monophyletic groups). Finally, we used HMMER (3.2.1) (67) to build hidden Markov model (HMM) protein profiles for each of the manually curated alignments, since two conserved regions were detected for the alignment of the T4CP family; as a result, two HMM profiles were built for *VirD4*. Finally, plasmid classification was performed using hmmsearch against the constructed HMM profiles, and the obtained homologs were further filtered based on the alignment length (covering more than 50% of the protein profile) and c value (< 0.01) (8). A type of MPF was attributed to a conjugative plasmid if the cluster contained at least five, four, four, and three type-specific markers for MPF_F, MPF_I, MPF_G, and MPF_T, respectively, in addition to the colocalization of ATPase and T4CP (8). All the constructed HMM profiles are available in ref. (68). We embedded a comprehensive structured AMR gene database (24 types, 1,208 subtypes) into our tool (69), and aligned the coding sequences of all the plasmids to this database using BLASTP (70) at *E* value $\leq 10^{-7}$ with a minimum similarity of 80% over 70% query coverage. In addition, a plasmid visualization component (71) using AngularJS was integrated into our tool to display the conjugative elements and the identified AMR genes. To evaluate the performance of Plascad, we used 44 conjugative plasmids, 22 mobilizable plasmids, and 39 nonmobilizable plasmids, which have been verified experimentally as the benchmark dataset (72) (Dataset S2). Receiver operating characteristic (ROC) analysis (sensitivity, specificity, and positive predictive value) was performed to assess the performance of Plascad. The final output of Plascad includes four files for the given plasmid sequences: 1) summary file of the plasmid classification result; 2) genetic location of the genes associated with plasmid transfer as well as the detected AMR genes for mobilizable and conjugative plasmids; and 3) HTML files containing the maps for all the identified conjugative plasmids. Plascad is a free open-source program implemented in Python3. It is available in GitHub (68).

Network Construction and MGEs Identification (ISs and Class 1 Integrons). AccNET was used to construct a bipartite network connecting plasmids (3,522) and AMR genes (73). The location of the plasmids and AMR genes was determined using ForceAtlas2 (24) as a force-directed layout algorithm (distance between nodes is relative and depends on forces of attraction and repulsion between the nodes). Gephi software (74) was used for network visualization and manipulation.

We were interested in exploring the contribution of additional MGEs that were associated with the resistance genes. Class 1 integrons (including both type A and type B) carried by plasmids were identified using the Integron Visualization and Identification Pipeline (I-VIP) with default settings (75). ISs were characterized based on homology search against the ISfinder database with BLASTN (*E* value $\leq 10^{-10}$) (76); the matches were further filtrated using thresholds for identity (80%) and coverage (80%); only the best hit (highest BLAST bit score) was selected for downstream analysis if multiple hits met these cutoffs. To study the association between ISs and AMR genes on plasmids, the adjacent sequences, i.e., 5 kb upstream and downstream of AMR genes, were extracted for the identification of ISs.

Identification of Recently Transferred AMR Genes and Toxin-Antitoxin Systems. The recently transferred AMR genes between plasmids and bacterial chromosomes were defined as the identical AMR genes (100% nucleotide identity and coverage) present on both plasmids and bacterial chromosomes identified using BLASTN (*E* value $\leq 10^{-5}$), and the recently transferred AMR genes in distantly related bacteria (defined as different genera) were investigated using the same approach. To investigate the influence of different plasmid categories (conjugative vs.. nonmobilizable) on the phylogenetic transfer range of AMR genes, we examined the taxonomy of bacteria hosting the AMR genes that were shared with conjugative plasmids, as well as those shared only with nonmobilizable plasmids. The phylogenetic tree was constructed with FastTree (v2.1.10) using a multiple sequence alignment generated by MUSCLE (v3.8.31) of the full length 16S rRNA gene sequences extracted from the complete genomes with Barrnap (v0.9) (77). Pathogenetic bacteria were identified with BLASTP (*E* value $\leq 10^{-10}$ with minimal identity and coverage of 80%) homology searches against the core VFDB dataset, which includes only genes associated with experimentally verified virulence factors (78). To identify the toxin-antitoxin systems, we used hmmsearch (alignment length >50% and c-value <0.01) against TASmania HMM profiles (79).

Determination of the Transfer Network Connecting IS-Associated AMR Genes between Plasmids and Bacterial Chromosomes. To demonstrate the contribution of ISs to the spread of AMR genes, we further restricted recent transfers to the presence of flanking ISs in addition to the shared AMR genes. The adjacent sequences (5 kb upstream and downstream of shared AMR genes) were extracted from both plasmids and bacterial chromosomes and searched against the ISfinder reference database using BLASTN (*E* value $\leq 10^{-10}$). In this case, the coverage was not considered as a cutoff for the identification of ISs, allowing the inclusion of ISs that may have been truncated due to their dynamic evolution, but the genetic arrangement of AMR genes and its adjacent associated ISs, i.e., same nucleotide distance between each AMR gene-IS pair in different genetic backgrounds, was used as an additional filter for the confirmation of IS-associated horizontal transfer. Finally, we measured all the transfer events for each AMR gene between each of the three plasmid categories and bacterial chromosomes. To avoid overcounting the number of transfers that are potentially vertically related, all genomic pairs sharing > 97% ANI were deduplicated using FastANI (80). To investigate the distributions of bacteria that were involved in the horizontal transfer of IS-associated AMR genes, normalization was conducted against the species level (only bacterial species with more than 20 genomes were considered) to avoid the bias caused by heterogeneous sequencing of pathogenic species.

In Vitro Experimental Reconstruction of IS-Associated (IS26) AMR Gene Transfer Mediated by Conjugative Plasmids (RP4).

Strains, plasmids, and media. The strains, plasmids, and concentrations of antibiotics used in this study are summarized in *SI Appendix*, Table S3.

Construction of the pUC57-IS26-Gm$^+$-IS26 and RP4-Plac-eyfp-Cat$^+$ plasmids, the E. coli K12 MC1061-Rif$^+$::lacI^q-Km$^+$, and E. coli K12 MC1061-Rif$^+$::mRuby3 strains. IS26-*Gm*$^+$-IS26 was synthesized [sequence available in ref. (81)] and cloned into the *Eco*RV site of the pUC57 plasmid. A gene cassette carrying a chloramphenicol resistance determinant and a *lacI*^{q} repressible promoter upstream of the *eyfp* gene was inserted into the RP4 plasmid in vitro by EZ-Tn5 transposase (Lucigen) following the manufacturer's instructions. K12 MC1061-*Rif*$^+$ was chromosomally tagged with a gene cassette (*lacI*^{q}-*K*$_m^+$) encoding kanamycin resistance and constitutive *lacI*^{q} production by the pGRG25 plasmid (*SI Appendix*). As a result, the expression of green/yellow fluorescent protein on the *eyfp*-tagged conjugative plasmid is inhibited in the donor strain, but expression is possible once the plasmid is transferred out of the donor strain, resulting in fluorescent cells, which can be detected by fluorescence microscopy. In addition, *mRuby3*-tagged *E. coli* K12 MC1061-*Rif*$^+$ was also constructed using the same method as described above.

Confirmation of IS26-mediated transposition in vitro. The transposition process was investigated via conjugation of the RP4-Plac-*eyfp*-*Cat*$^+$ plasmid into *E. coli* DH5α cells containing the nonconjugative plasmid pUC57-IS26-*Gm*$^+$-IS26. Cointegrates were determined by mating with the *E. coli* K12 MC1061-*Rif*$^+$ strain and selecting for *Rif* ^{R} *Gm*^{R} *Tet*^{R} *Cat*^{R} fluorescent colonies. To investigate the stability of the mechanism and the fate of *Gm*^{R} after the conjugation process, the three resulting cointegrates obtained above were then introduced into *E. coli* K12 MC1061-*Rif*$^+$::*mRuby3* (red fluorescence) by a further mating assay. Finally, nanopore sequencing was performed to confirm the genetic locations of the IS26-mediated incorporation of *Gm*^{R} into the *eyfp*-tagged RP4 plasmid and the chromosomes of *E. coli* DH5α and *E. coli* K12 MC1061-*Rif*$^+$::*mRuby3* (*SI Appendix*).

Confirmation of IS26-associated AMR gene transfer mediated by the RP4 plasmid in indigenous bacterial communities of AS samples collected from two WWTPs. To provide further evidence of the extraordinary capability of interaction between conjugative plasmids and ISs in facilitating the spread of AMR genes in complex bacterial communities, we reproduced the gene transfer process experimentally. A mating assay was conducted between the indigenous recipient communities collected from each of the two AS samples, i.e.,Shatin (ST) andShek Wu Hui (SWH), and the donor bacteria (*E. coli* K12 MC1061-*Rif*$^+$::*lacI*^{q}-*K*$_m^+$) harboring the cointegrated RP4 plasmid (RP4-Plac-*eyfp*-*cat*$^+$-IS26-*Gm*$^+$-IS26). The transconjugants (*Tet*^{R} *Cat*^{R} *Gm*^{R}) on the selection media were characterized by fluorescence microscopy. Ten transconjugants were randomly picked from each experiment and sequenced by nanopore sequencing to investigate the fate of the RP4 plasmid as well as the IS26-associated *Gm*^{R} (*SI Appendix*).

Nanopore sequencing and data analysis. The sequencing library preparation was performed using the SQK-RBK004 Rapid Barcoding Kit (nanopore) following the manufacturer's instructions, and then, GridION sequencing was performed using R9.4 flow cells for 48 h. The statistics of the sequencing reads are summarized in *SI Appendix*, Table S4. Raw reads were base called and demultiplexed using Guppy 3.0.3 (https://community.nanoporetech.com) to return separate fastq files. Reads were aligned to the reference sequences of the RP4 plasmid, *E. coli* DH5α, and *E. coli* K12 MC1061-*Rif*$^+$ using Minimap2 (82) and BLASTN (*E* value $\leq 10^{-7}$) to determine the positions of the cointegrate junctions. For the 20 transconjugants, base-called reads were first

assembled with Unicycler (83), and the resulting draft genomes were polished using Medaka (84). The genetic location of the IS26-associated Gm^R on the chromosomes of transconjugants was determined by mapping the base-called reads to the assemblies.

Data Availability. The base-called Nanopore reads were deposited into the NCBI SRA database with the following accession number: PRJNA558442. Plascad is available in GitHub (https://github.com/pianpianyouche/plascad) (68). IS26-Gm^+-IS26 sequence is available in Figshare (https://doi.org/10.6084/m9.figshare.13107803.v1) (81).

ACKNOWLEDGMENTS. Y.C., Y.Y., and X.X. thank The University of Hong Kong for the postgraduate studentship. We thank Prof. Philip Hugenholtz from Australian Centre for Ecogenomics for his suggestions in data analysis. We appreciate the help of Vicky and thank Lilian Y. L. Chan for the technical assistance with the High Performance Computing & Grid Computing system. This work was supported by the State Key Laboratory of Marine Pollution Seed Collaborative Research Fund (SCRF/0023) and partially supported by a grant from the Research Grants Council of Hong Kong Special Administrative Region, China (Project No. T21-705/20-N).

1. D. I. Andersson, D. Hughes, Antibiotic resistance and its cost: Is it possible to reverse resistance? *Nat. Rev. Microbiol.* **8**, 260–271 (2010).
2. E. Wistrand-Yuen *et al*., Evolution of high-level resistance during low-level antibiotic exposure. *Nat. Commun.* **9**, 1599 (2018).
3. A. San Millan, Evolution of plasmid-mediated antibiotic resistance in the clinical context. *Trends Microbiol.* **26**, 978–985 (2018).
4. P. M. Bennett, Plasmid encoded antibiotic resistance: Acquisition and transfer of antibiotic resistance genes in bacteria. *Br. J. Pharmacol.* **153** (suppl. 1), S347–S357 (2008).
5. P. Bradley, H. C. den Bakker, E. P. C. Rocha, G. McVean, Z. Iqbal, Ultrafast search of all deposited bacterial and viral genomic data. *Nat. Biotechnol.* **37**, 152–159 (2019).
6. C. Smillie, M. P. Garcillán-Barcia, M. V. Francia, E. P. C. Rocha, F. de la Cruz, Mobility of plasmids. *Microbiol. Mol. Biol. Rev.* **74**, 434–452 (2010).
7. M. P. Garcillán-Barcia, M. V. Francia, F. de la Cruz, The diversity of conjugative relaxases and its application in plasmid classification. *FEMS Microbiol. Rev.* **33**, 657–687 (2009).
8. J. Guglielmini, L. Quintais, M. P. Garcillán-Barcia, F. de la Cruz, E. P. C. Rocha, The repertoire of ICE in prokaryotes underscores the unity, diversity, and ubiquity of conjugation. *PLoS Genet.* **7**, e1002222 (2011).
9. R. Fernandez-Lopez, S. Redondo, M. P. Garcillan-Barcia, F. de la Cruz, Towards a taxonomy of conjugative plasmids. *Curr. Opin. Microbiol.* **38**, 106–113 (2017).
10. A. Orlek *et al*., Plasmid classification in an Era of whole-genome sequencing: Application in studies of antibiotic resistance epidemiology. *Front. Microbiol.* **8**, 182 (2017).
11. A. Orlek *et al*., Ordering the mob: Insights into replicon and MOB typing schemes from analysis of a curated dataset of publicly available plasmids. *Plasmid* **91**, 42–52 (2017).
12. J. Robertson, J. H. E. Nash, MOB-suite: Software tools for clustering, reconstruction and typing of plasmids from draft assemblies. *Microb. Genom.* **4**, e000206 (2018).
13. J. Robertson, K. Bessonov, J. Schonfeld, J. H. E. Nash, Universal whole-sequence-based plasmid typing and its utility to prediction of host range and epidemiological surveillance. *Microb. Genom.* **6**, mgen000435 (2020).
14. D. R. Evans *et al*., Systematic detection of horizontal gene transfer across genera among multidrug-resistant bacteria in a single hospital. *Elife* **9**, e53886 (2020).
15. M. Rozwandowicz *et al*., Plasmids carrying antimicrobial resistance genes in Enterobacteriaceae. *J. Antimicrob. Chemother.* **73**, 1121–1137 (2018).
16. M. Tamminen, M. Virta, R. Fani, M. Fondi, Large-scale analysis of plasmid relationships through gene-sharing networks. *Mol. Biol. Evol.* **29**, 1225–1240 (2012).
17. D. Mazel, Integrons: Agents of bacterial evolution. *Nat. Rev. Microbiol.* **4**, 608–620 (2006).
18. M. D. Adams, B. Bishop, M. S. Wright, Quantitative assessment of insertion sequence impact on bacterial genome architecture. *Microb. Genom.* **2**, e000062 (2016).
19. M. Shintani, Z. K. Sanchez, K. Kimbara, Genomics of microbial plasmids: Classification and identification based on replication and transfer systems and host taxonomy. *Front. Microbiol.* **6**, 242 (2015).
20. R. El-Awady *et al*., The role of eukaryotic and prokaryotic ABC transporter family in failure of chemotherapy. *Front. Pharmacol.* **7**, 535 (2017).
21. A. U. Khan, L. Maryam, R. Zarrilli, Structure, genetics and worldwide spread of New Delhi metallo-β-lactamase (NDM): A threat to public health. *BMC Microbiol.* **17**, 101 (2017).
22. E. R. Bevan, A. M. Jones, P. M. Hawkey, Global epidemiology of CTX-M β-lactamases: Temporal and geographical shifts in genotype. *J. Antimicrob. Chemother.* **72**, 2145–2155 (2017).
23. R. Wang *et al*., The global distribution and spread of the mobilized colistin resistance gene mcr-1. *Nat. Commun.* **9**, 1179 (2018).
24. M. Jacomy, T. Venturini, S. Heymann, M. Bastian, ForceAtlas2, a continuous graph layout algorithm for handy network visualization designed for the Gephi software. *PLoS One* **9**, e98679 (2014).
25. A. Norman, L. H. Hansen, S. J. Sørensen, Conjugative plasmids: Vessels of the communal gene pool. *Philos. Trans. R. Soc. Lond. B Biol. Sci.* **364**, 2275–2289 (2009).
26. C. M. Thomas, K. M. Nielsen, Mechanisms of, and barriers to, horizontal gene transfer between bacteria. *Nat. Rev. Microbiol.* **3**, 711–721 (2005).
27. S. Redondo-Salvo *et al*., Pathways for horizontal gene transfer in bacteria revealed by a global map of their plasmids. *Nat. Commun.* **11**, 3602 (2020).
28. C. S. Smillie *et al*., Ecology drives a global network of gene exchange connecting the human microbiome. *Nature* **480**, 241–244 (2011).
29. S. Hernando-Amado, T. M. Coque, F. Baquero, J. L. Martínez, Defining and combating antibiotic resistance from one health and global health perspectives. *Nat. Microbiol.* **4**, 1432–1442 (2019).
30. M. Gillings *et al*., The evolution of class 1 integrons and the rise of antibiotic resistance. *J. Bacteriol.* **190**, 5095–5100 (2008).
31. P. H. Oliveira, M. Touchon, J. Cury, E. P. C. Rocha, The chromosomal organization of horizontal gene transfer in bacteria. *Nat. Commun.* **8**, 841 (2017).
32. M. Kusumoto *et al*., Insertion sequence-excision enhancer removes transposable elements from bacterial genomes and induces various genomic deletions. *Nat. Commun.* **2**, 152 (2011).
33. B. J. Woodcroft *et al*., Genome-centric view of carbon processing in thawing permafrost. *Nature* **560**, 49–54 (2018).
34. M. S. Mulani, E. E. Kamble, S. N. Kumkar, M. S. Tawre, K. R. Pardesi, Emerging strategies to combat ESKAPE pathogens in the era of antimicrobial resistance: A review. *Front. Microbiol.* **10**, 539 (2019).
35. S. R. Partridge, S. M. Kwong, N. Firth, S. O. Jensen, Mobile genetic elements associated with antimicrobial resistance. *Clin. Microbiol. Rev.* **31**, e00088-17 (2018).
36. S. R. Partridge, Analysis of antibiotic resistance regions in Gram-negative bacteria. *FEMS Microbiol. Rev.* **35**, 820–855 (2011).
37. L. Dortet, L. Poirel, P. Nordmann, Worldwide dissemination of the NDM-type carbapenemases in Gram-negative bacteria. *BioMed Res. Int.* **2014**, 249856 (2014).
38. T. Naas *et al*., Genetic structures at the origin of acquisition of the beta-lactamase bla $_{KPC}$ gene. *Antimicrob. Agents Chemother.* **52**, 1257–1263 (2008).
39. C. J. Harmer, R. A. Moran, R. M. Hall, Movement of IS26-associated antibiotic resistance genes occurs via a translocatable unit that includes a single IS26 and preferentially inserts adjacent to another IS26. *mBio* **5**, e01801-14 (2014).
40. S. Halary, J. W. Leigh, B. Cheaib, P. Lopez, E. Bapteste, Network analyses structure genetic diversity in independent genetic worlds. *Proc. Natl. Acad. Sci. U.S.A.* **107**, 127–132 (2010).
41. U. Klümper *et al*., Broad host range plasmids can invade an unexpectedly diverse fraction of a soil bacterial community. *ISME J.* **9**, 934–945 (2015).
42. L. Li *et al*., Estimating the transfer range of plasmids encoding antimicrobial resistance in a wastewater treatment plant microbial community. *Environ. Sci. Technol. Lett.* **5**, 260–265 (2018).
43. E. Grohmann, G. Muth, M. Espinosa, Conjugative plasmid transfer in gram-positive bacteria. *Microbiol. Mol. Biol. Rev.* **67**, 277–301 (2003).
44. H. Xue *et al*., Eco-Evolutionary dynamics of episomes among ecologically cohesive bacterial populations. *mBio* **6**, e00552-15 (2015).
45. H. Ochman, J. G. Lawrence, E. A. Groisman, Lateral gene transfer and the nature of bacterial innovation. *Nature* **405**, 299–304 (2000).
46. R. Page, W. Peti, Toxin-antitoxin systems in bacterial growth arrest and persistence. *Nat. Chem. Biol.* **12**, 208–214 (2016).
47. L. Van Melderen, Toxin-antitoxin systems: Why so many, what for? *Curr. Opin. Microbiol.* **13**, 781–785 (2010).
48. B. Li *et al*., Metagenomic and network analysis reveal wide distribution and co-occurrence of environmental antibiotic resistance genes. *ISME J.* **9**, 2490–2502 (2015).
49. L. Ma *et al*., Catalogue of antibiotic resistome and host-tracking in drinking water deciphered by a large scale survey. *Microbiome* **5**, 154 (2017).
50. F. Ju *et al*., Wastewater treatment plant resistomes are shaped by bacterial composition, genetic exchange, and upregulated expression in the effluent microbiomes. *ISME J.* **13**, 346–360 (2019).
51. M. N. Alekshun, S. B. Levy, Molecular mechanisms of antibacterial multidrug resistance. *Cell* **128**, 1037–1050 (2007).
52. D. Du *et al*., Multidrug efflux pumps: Structure, function and regulation. *Nat. Rev. Microbiol.* **16**, 523–539 (2018).
53. C. J. Harmer, R. M. Hall, IS26-mediated precise excision of the IS26-aphA1a translocatable unit. *mBio* **6**, e01866-15 (2015).
54. A. San Millan *et al*., Integrative analysis of fitness and metabolic effects of plasmids in Pseudomonas aeruginosa PAO1. *ISME J.* **12**, 3014–3024 (2018).
55. G. Cuzon, T. Naas, P. Nordmann, Functional characterization of Tn4401, a Tn3-based transposon involved in blaKPC gene mobilization. *Antimicrob. Agents Chemother.* **55**, 5370–5373 (2011).
56. A. San Millan *et al*., Positive selection and compensatory adaptation interact to stabilize non-transmissible plasmids. *Nat. Commun.* **5**, 5208 (2014).
57. M.-F. Lartigue, L. Poirel, D. Aubert, P. Nordmann, In vitro analysis of ISEcp1B-mediated mobilization of naturally occurring beta-lactamase gene blaCTX-M of Kluyvera ascorbata. *Antimicrob. Agents Chemother.* **50**, 1282–1286 (2006).
58. M. J. Bottery, A. J. Wood, M. A. Brockhurst, Temporal dynamics of bacteria-plasmid coevolution under antibiotic selection. *ISME J.* **13**, 559–562 (2019).
59. A. J. Lopatkin *et al*., Antibiotics as a selective driver for conjugation dynamics. *Nat. Microbiol.* **1**, 16044 (2016).
60. T. Charalampous *et al*., Nanopore metagenomics enables rapid clinical diagnosis of bacterial lower respiratory infection. *Nat. Biotechnol.* **37**, 783–792 (2019).
61. Y. Che *et al*., Mobile antibiotic resistome in wastewater treatment plants revealed by Nanopore metagenomic sequencing. *Microbiome* **7**, 44 (2019).

62. D. H. Parks *et al*., A standardized bacterial taxonomy based on genome phylogeny substantially revises the tree of life. *Nat. Biotechnol.* **36**, 996–1004 (2018).
63. S. F. Altschul *et al*., Gapped BLAST and PSI-BLAST: A new generation of protein database search programs. *Nucleic Acids Res.* **25**, 3389–3402 (1997).
64. D. Hyatt *et al*., Prodigal: Prokaryotic gene recognition and translation initiation site identification. *BMC Bioinformatics* **11**, 119 (2010).
65. R. C. Edgar, MUSCLE: Multiple sequence alignment with high accuracy and high throughput. *Nucleic Acids Res.* **32**, 1792–1797 (2004).
66. M. N. Price, P. S. Dehal, A. P. Arkin, FastTree 2–Approximately maximum-likelihood trees for large alignments. *PLoS One* **5**, e9490 (2010).
67. S. R. Eddy, Accelerated profile HMM searches. *PLoS Comput. Biol.* **7**, e1002195 (2011).
68. Y. Che, Plascad. GitHub. https://github.com/pianpianyouche/plascad. Deposited 16 September 2020.
69. X. Yin *et al*., ARGs-OAP v2.0 with an expanded SARG database and Hidden Markov Models for enhancement characterization and quantification of antibiotic resistance genes in environmental metagenomes. *Bioinformatics* **34**, 2263–2270 (2018).
70. C. Camacho *et al*., BLAST+: Architecture and applications. *BMC Bioinformatics* **10**, 421 (2009).
71. R. Chawdry, Data from "AngularPlasmid." GitHub. https://github.com/vixis/angularplasmid. Accessed 21 January 2021.
72. X. Li *et al*., oriTfinder: a web-based tool for the identification of origin of transfers in DNA sequences of bacterial mobile genetic elements. *Nucleic Acids Res.* **46**, W229–W234 (2018).
73. V. F. Lanza, F. Baquero, F. de la Cruz, T. M. Coque, AcCNET (accessory genome constellation network): Comparative genomics software for accessory genome analysis using bipartite networks. *Bioinformatics* **33**, 283–285 (2017).
74. M. Bastian, S. Heymann, M. Jacomy, "Gephi: An open source software for exploring and manipulating networks" in *International AAAI Conference on Weblogs and Social Media* (AAAI Press, Menlo Park, CA, 2009).
75. A. N. Zhang *et al*., Conserved phylogenetic distribution and limited antibiotic resistance of class 1 integrons revealed by assessing the bacterial genome and plasmid collection. *Microbiome* **6**, 130 (2018).
76. P. Siguier, J. Perochon, L. Lestrade, J. Mahillon, M. Chandler, ISfinder: The reference centre for bacterial insertion sequences. *Nucleic Acids Res.* **34**, D32–D36 (2006).
77. T. Seemann, Data from "Barrnap." GitHub. https://github.com/tseemann/barrnap. Accessed 21 January 2021.
78. B. Liu, D. Zheng, Q. Jin, L. Chen, J. Yang, VFDB 2019: A comparative pathogenomic platform with an interactive web interface. *Nucleic Acids Res.* **47**, D687–D692 (2019).
79. H. Akarsu *et al*., TASmania: A bacterial toxin-antitoxin systems database. *PLoS Comput. Biol.* **15**, e1006946 (2019).
80. C. Jain, L. M. Rodriguez-R, A. M. Phillippy, K. T. Konstantinidis, S. Aluru, High throughput ANI analysis of 90K prokaryotic genomes reveals clear species boundaries. *Nat. Commun.* **9**, 5114 (2018).
81. Y. Che, IS26-gm-IS26 gene cluster. *Figshare*. https://doi.org/10.6084/m9.figshare.13107803.v1. Deposited 20 October 2020.
82. H. Li, Minimap2: Pairwise alignment for nucleotide sequences. *Bioinformatics* **34**, 3094–3100 (2018).
83. R. R. Wick, L. M. Judd, C. L. Gorrie, K. E. Holt, Unicycler: Resolving bacterial genome assemblies from short and long sequencing reads. *PLoS Comput. Biol.* **13**, e1005595 (2017).
84. Oxford Nanopore Technologies, Data from "Medaka." GitHub. https://github.com/nanoporetech/medaka. Accessed 21 January 2021.